Olive mill wastewater: From a pollutant to green fuels, agricultural and water source and bio-fertilizer -Hydrothermal carbonization

Ahmed Amine Azzaz, Mejdi Jeguirim, Vasiliki Kinigopoulou, Charalampos Doulgeris, Mary-Lorène Goddard, Salah Jellali, Camelia Ghimbeu

HAL Id: hal-03060287
https://hal.archives-ouvertes.fr/hal-03060287

Submitted on 17 Dec 2020

Olive Mill Wastewater: From a Pollutant to Green Fuels, Agricultural and Water Source and Bio-Fertilizer – Hydrothermal Carbonization

Ahmed Amine Azzaz [a,b,*]**, Mejdi Jeguirim** [a,b]**, Vasiliki Kinigopoulou** [c]**, Charalampos Doulgeris** [c]**, Mary-Lorène Goddard** [d,e,] **Salah Jellali** [f]**, Camelia Matei Ghimbeu** [a,b]

a Université de Haute-Alsace, CNRS, Institut de Science des Matériaux de Mulhouse (IS2M) UMR 7361, F-68100 Mulhouse, France
b Université de Strasbourg, F-67081 Strasbourg, France
c Soil & Water Resources Institute, Hellenic Agricultural Organisation "DEMETER", Sindos, Central Macedonia 57400, Greece
d Université de Haute-Alsace, Université de Strasbourg, CNRS, LIMA UMR 7042, Mulhouse, France
e Université de Haute-Alsace, LVBE, EA-3991 Colmar, France
f PEIE Research Chair for the Development of Industrial Estates and Free Zones, Center for Environmental Studies and Research (CESAR), Sultan Qaboos University, Al-Khoud, 123 Muscat, Oman

Abstract

Hydrothermal carbonization (HTC) is considered as a promising technique for wastes conversion into carbon rich materials for various energetic, environmental and agricultural applications. In this work, the HTC of olive mill wastewater (OMWW) was investigated at different temperatures (180 – 220°C) and both, the solid (i.e., hydrochars) and the final process liquid derived from the thermal conversion process were deeply analyzed. Results showed that the solid yield was affected by the temperature, i.e., decrease from 57% to 25% for temperatures of 180°C and 220°C, respectively. Furthermore, the hydrochars presented an increasing fixed carbon percentage with the increase of the carbonization temperature, suggesting that decarboxylation is the main reaction driving the HTC process. The decrease in the O/C ratio promoted an increase of the high heating value (HHV) by 32% for hydrochar prepared at 220°C. The process liquids were sampled and their organic contents were analyzed using GC-MS technique. Acids, alcohols, phenols and sugar derivatives were detected and their concentrations varied with carbonization temperatures. The assessment of the physico-chemical properties of the generated HTC by-products suggested the possible application of the hydrochars for energetic insights while the liquid fraction could be practical for in agricultural field.

Keywords: Hydrothermal carbonization, Olive Mill Wastewater, Hydrochars, biofuels, characterization, Mineral content, HHV.

1. Introduction

The cultivation of olive trees was practiced for millennials in the Mediterranean region. According to the FAO (Food and Agriculture Organization, 2017), 16.8 million ha of harvested area in the Mediterranean basin generated about 95% of the worldwide olive production. Such intensive activity has positive impact on the concerned countries' economies (such as Tunisia, Spain, Greece and Italy). In fact, 5.8 million people are directly and indirectly life-depending on this agricultural field, where 53% of them are classified among the disadvantaged population (International Labor Organization, 2017).

In Tunisia, the olive oil production in the 2017/2018 season was valued to 280,000 tons (Food and Agriculture Organization, 2017). Despite its significant contribution to the national assets, the oleic industries use the three-phases milling method that was prohibited in Spain since 1972. This milling technique is characterized by the production of solid and liquid wastes at considerable amounts (Chouchene et al., 2012). The solid fraction, namely olive raw pomace (ROP) is widely employed in the amendment of soils, animals feeding and bio-energy production (Moreno-Maroto et al., 2019). However, the liquid fraction, olive mill wastewater (OMWW), is poorly exploited since it is considered as economically and environmentally problematic. In fact, OMWW is an environmentally-critical-effluent due to its high organic matter and toxic monophenolic compounds contents (Aktas et al., 2001). Currently, these liquids are improperly treated, being left-out in outdoor storage/evaporation lagoons. During the periods of high precipitations, they could reach water bodies and cause serious modifications to the underground water properties (Souilem et al., 2017). Additionally, their acidic pH, high electrical conductivity and content in organic matter could noticeably affect the soil and underground water quality (Doula et al., 2013). Along with these parameters, total nitrogen, exchangeable phosphorus and potassium contents figure as "double role" factors. In

fact, these nutrients are decisive to increase the agricultural soils fertility but their excessive presence in porous media could alter its overall ionic equilibrium (Komnitsas and Zaharaki, 2012).

Several studies have investigated the treatment of this so-called "burden" by various treatment techniques. They include biological, advanced oxidation and physico-chemical methods (Azzaz et al., 2020; Chatzisymeon et al., 2013; Fezzani and Cheikh, 2010; Hodaifa et al., 2013; Lucas and Peres, 2009; Pulido, 2016; Sedej et al., 2016; Yalili Kiliç et al., 2013; Zirehpour et al., 2012) The main advantages and inconvenient of these techniques are detailed in Table S1 (Supplementary Information). Generally, these methods aim to recover water from OMWW without taking into account the intriguing potentials of this waste as a whole entity. Recently, Haddad *et al.* (2017) proposed the thermal conversion of these liquid organic wastes, after impregnation on dry biomass, by slow pyrolysis at 500°C. They produced a biochar rich in phosphorus and nitrogen, with a low amount of volatile fraction and a high porosity media. The produced biochar was applied as biofertilizer and showed an equaled impact on the growth of rye grass leaves when compared to a commercial fertilizer (Haddad et al., 2017). These results were encouraging to go forward in this research direction. Nonetheless, the OMWW is a 90% water composed waste. Therefore, the pyrolysis reaction (which is already performed at high temperature) had to be preceded by a preliminary drying step, thus significantly inflating the treatment costs (Jeguirim et al., 2017). Moreover, thermal treatment at high temperature resulted in low final solid yield which limits their production at large scale.

Alternatively, the hydrothermal carbonization is a thermal process allowing the conversion of liquid or wet-solid-wastes into carbonaceous materials (called hydrochars) with appreciable yields (Wang et al., 2018). These hydrochars present interesting physico-chemical and energetic characteristics that could be exploited in a wide range of applications (Kruse and Dahmen, 2018). Moreover, the hydrochars production process consumes low energy compared to the

slow pyrolysis method which explains their relatively low market price compared to biochars (Saba et al., 2019). The use of hydrochars as bio-fertilizers was investigated, owing to their important contents in minerals as well as the relatively slow carbon sequestration compared to biochars (Naisse et al., 2015). Hydrochars could also enhance the development of crops, as well as the quality and sustainability of the low-fertile soils (Bargmann et al., 2014, 2013; Dieguez-Alonso et al., 2018; Gajić et al., 2012). Other investigations tried to improve the hydrochars properties by increasing their specific surface area and porosities through chemical and/or physical activations. The resulting activated carbons were successfully applied for the removal of various pollutants from aqueous solutions (Xue et al., 2012; Zuo et al., 2016), air (Hao et al., 2016; Zhang et al., 2019) and soils (Chung et al., 2015; Kammann et al., 2012). Moreover, various researchers have increased the hydrochars specific surface area after thermal treatment at higher temperatures (Fang et al., 2016; Yu et al., 2019). These thermally treated hydrochars could present singular carbon nano-sphere forms, commonly employed for the synthesis of electrodes in supercapacitors and batteries, for the storage of gases and electricity (Kim et al., 2015; Unur et al., 2013).

The use of HTC process for the treatment of olive mill wastes in Spain (Benavente et al., 2017), Turkey (Donar et al., 2016) and Italy (Volpe et al., 2018) has been only recently investigated. Even if these countries use the two phases milling method, the physico-chemical characteristics of the related produced hydrochars were very different, especially in terms of content in carbon and minerals, energetic aspect and structural morphologies. This could be attributed to the difference in the properties of the used feedstocks. To the best of our knowledge, the use of the HTC process as a sustainable recovery method for the OMWW generated by the three phase mills (case of Tunisia, Algeria and Morocco) were not yet performed. Therefore, a deep characterization of Tunisian OMWW based hydrochars was performed through their structure, morphology, surface chemistry and nutrients contents

analyses. Furthermore, the organic and the mineral contents of the liquid fraction generated during the HTC of OMMWW were determined using various analytical techniques. Such characterizations will help to predict the potential of OMWW's HTC by-products in energetic, agricultural and/or environmental applications.

2. Materials and methods

2.1. Olive Mill Wastewater and the corresponding Solid Fraction

The used olive mill wastewater (OMWW) was collected from a local olive mill plant at the region of Touta, north east of Tunisia. It was stored in plastic bins and used in the following experiments without any performed treatments or purifications.

The solid phase of the used olive mill wastewater was separated from the liquid one by vacuum filtration by using a 0.45 µm Whatman® filter paper (VWR, Leuven, Belgium). The percentage of dried solid content was determined according to the TAPPI/ANSI T 412 om-16 method (T-412, 2012) described as follows: 10 g of OMWW was weighted in a glass crucible then introduced in an oven at 120°C for 48h. The remaining mass presents the solid fraction and the difference is the content in water. Results showed that solid fraction contained in the used OMWW is estimated to about 7.9%. This solid phase, labeled as $OMWW_{SF}$, was fully characterized by using several analytical equipment (see section 2.4).

2.2. Hydrochar synthesis

The HTC of the OMWW was carried out using a high-pressure laboratory autoclave (Top Industrie, Vaux-le-Pénil, France). During these assays, 10 mL of OMWW were heated at three different temperatures 180, 200 and 220°C for constant heating rate and residence time of 10°C/min and 24 h, respectively. The produced hydrochars were named as follows: T- OMWW, where T is the carbonization temperature (°C). After carbonization, the corresponding mixtures

were filtered and the solid phases were dried in an oven at 105°C overnight and then weighted

and stored in glass vials.

For a given experiment, the produced hydrochar yield (Y_{HC}, %) was calculated as follows:

$$Y_{HC}(\%) = m_{HC}/m_{OMWWSF} \times 100 \qquad \text{(Eq. 1)}$$

where m_{HC} (g) is the recovered dry solid mass after carbonization and m_{OMWWSF} is the initial

$OMWW_{SF}$ feedstock mass (g).

2.3. Hydrochars and OMWW$_{SF}$ characterization

The characterization of the $OMWW_{SF}$ as well as the produced hydrochars issued from the

OMWW hydrothermal carbonization at different temperatures were performed using different

analytical techniques:

2.3.1. Proximate, elemental and minerals content analyses

A TGA/DSC3+ apparatus (Mettler-Toledo, Greifense, Switzerland) was used for the

proximate analysis of the hydrochars and the $OMWW_{SF}$ according to the TGA procedure

(Jeguirim et al., 2014).

The elemental analysis was performed in order to determine the solid phases contents in

terms of C, H, N, O and S. It was assessed by using a Flash 2000 CHNS-O elemental analyzer

(Thermo Scientific, Cambridge, UK).

The minerals compositions of the $OMWW_{SF}$ and the hydrochars were determined by using

the multiple extraction methods described by Thomson and Leege (Thompson and Leege,

1998), for the determination of water soluble phosphorus and magnesium, calcium, sodium,

potassium and ammonium nitrogen. In order to determine the total nitrogen in the samples,

modified Kjeldahl method was employed according to the ISO 11261 protocol (International Organization for Standardization, 1995).

2.3.2. Structure and morphology

Powder X-Ray diffraction (XRD) analysis was employed to identify the crystalline phases. It was carried out by a Panalytical X'Pert powder diffractometer (Malvern, UK) equipped with a copper anode. Phases identification was performed using the international center for diffraction data (ICDD) database available on the Panalytical Highscore software (Graulis et al., 2009).

Scanning electronic microscopy (SEM) analysis was performed using a XL30 electron microscope (Philips, Eindhoven, Netherlands) in order to assess the hydrochars morphology. Elementary composition of the materials was determined through an Energy-dispersive X-Ray spectrometer (X-Sight EDX model; Oxford Instruments, Oxfordshire, UK).

2.3.3. Surface chemistry

In order to predict the dominating surface charge of the obtained hydrochars, pH_{ZPC} value was determined using the method described in the literature (Azzaz et al., 2015). In particular, 0.2 g of each solid is immerged in a 0.1 M NaCl (VWR, Paris, France) solution at different initial pH (2 to 12). The plot $\Delta pH = pH_{initial} - pH_{final}$ vs. $pH_{initial}$ was depicted and the pH_{ZPC} value was described as its intersection point with the horizontal axis.

On the other hand, the determination of the main surface functional groups was assessed using the Boehm titration method for the oxygenic functions determination (Boehm, 2002). During this titration, 1 g of each feedstock and hydrochar were introduced in round-bottom flasks containing 50 mL of NaOH (Sigma Aldrich, Steinheim, Germany), Na_2CO_3 (SDS, Peypin, France) and $NaHCO_3$ (Merck, Darmstadt, Germany) at 0.1M. The choice of these

reagents is based on the assumption that NaOH neutralizes phenolic, lactonic, and carboxylic acids, NaHCO$_3$ neutralizes the carboxylic and lactonic groups and finally Na$_2$CO$_3$ neutralizes the carboxylic acids. The followed solid samples were kept in continuous stirring (200 rpm, 20°C ± 2 °C) for 24 h under argon gas flow of 15 NL/h to evacuate possible CO$_2$ emission. Aliquots were then recovered and filtered using 0.2 μm polypropelene syringe filters (VWR, Leuven, Belgium) then back-titrated using 0.05M of HCl solutions (Sigma Aldrich, Steinheim, Germany).

Infrared spectroscopy was used to identify the main functional groups present on the hydrochars' surface. The acquisition of the FTIR spectra was performed with an Equinox 55, Brucker spectrometer (Ettlingen, Germany). For each sample, a solid mass to KBr ratio of 1/200 was ground in a mortar and pressed into 1cm diameter disk with 3.5 tons pressure. The disk-like sample was then analyzed at a spectral resolution of 4 cm^{-1}, measured between 4000 and 400 cm^{-1}.

2.3.4. Energy contents

The higher heating values (HHV, MJ/kg) was determined using a C200 bomb calorimeter (IKA, Staufen, Germany) according to the DIN 51900-3 protocol (DIN, 2005) at adiabatic reaction mode. The lower heating values (LHV, MJ/kg) related to the released energy during the combustion of a solid without taking into account the energy of water condensation. The LHV were calculated on the basis of the values of the HHV and the percentages of moisture and hydrogen (at dry base).

2.3.5. Liquid Characterization

The chemical oxygen demand of the residual liquid phase after the HTC of the OMWW (COD; g O$_2$/L) was determined as an indicator of their organic matter content. It was assessed via the open reflux using dichromate titrimetric method (Allan Moore et al., 1949).

1   The total content of minerals in the residual liquid after the HTC was determined by

2   using an ARCOS ICP-OES analyzer (SPECTRO, Kleve, Germany). Samples were digested for

3   30 min with 5 mL of concentrated nitric acid and 1mL of 30% (v/v) oxygen peroxide at boiling

4   water and measurements were performed in synchronous mode.

5   The liquid recovery ratio for the studied minerals was estimated compared to the initial

6   concentrations present in the liquid fraction of OMWW according to the following equation:

7    $R_{minerals}(\%) = \frac{C_{i,OMWW} - C_{t,T-OMWW}}{C_{i,OMWW}} \times 100$ (Eq. 2)

8   Where $C_{i,OMWW}$ is the initial concentration of the mineral (K, Na, Ca, Mg, P and N) in

9   OMWW liquid fraction that was recovered after vacuum pump filtration and $C_{i,T-OMWW}$ is the

10   final concentration of minerals in the liquid fraction at a given T temperature after HTC.

11   Organic compounds in the liquid part of OMWW and T-OMWW (T = 180, 200 and

12   220°C) was determined using a GC-2010 gas chromatograph coupled with GC-QP2010 mass

13   detector (Shimadzu, Tokyo, Japan). Samples were initially filtered at 0.2 μm with regenerated

14   cellulose syringe filters then diluted 10 times in ultra-pure water (at a given resistivity of 18.0

15   MΩ cm). Afterwards, 30 μL of the diluted solutions were mixed in a vial with 50 μL of 10

16   μg/mL phenoxyacetic acid solution as internal standard. After lyophilization process, each

17   sample was derivatized and analysed by GC-MS according to the protocol described in a

18   previous paper (Jeguirim et al., 2020). The annotation of different peak was performed by using

19   a personal library of commercial compounds along with mass spectral library NIST 17.

20   **3. Results**

21   **3.1. Carbonization Yields**

22   The apparent aspects and yields production of hydrochars at different temperatures are

23   presented in Figure 1. The hydrochars aspect changed gradually with temperature from light

brown (for OMWW) to black (for 220-OMWW) with more voluminous conglomerates. It is

also observed that hydrochar production yields decrease with the carbonization temperature

from 57% at 180°C to 25% at 220°C. In fact, the increase in treatment temperature enhances

significantly the heat gradient inside the autoclave and thereby affects the biomass inner

structure (Zhang et al., 2014). According to Hoekmann et *al.* (2011), the modification

intensifies with higher energy intake, as the biomass undergoes a successive degradation

towards the polymerization of large molecules. Moreover, the outer structure could be affected

by the volatile matter reduction accompanied in the same time with the dehydration and

decarboxylation of cellulose and lignin matrices (Ruiz et al., 2013).
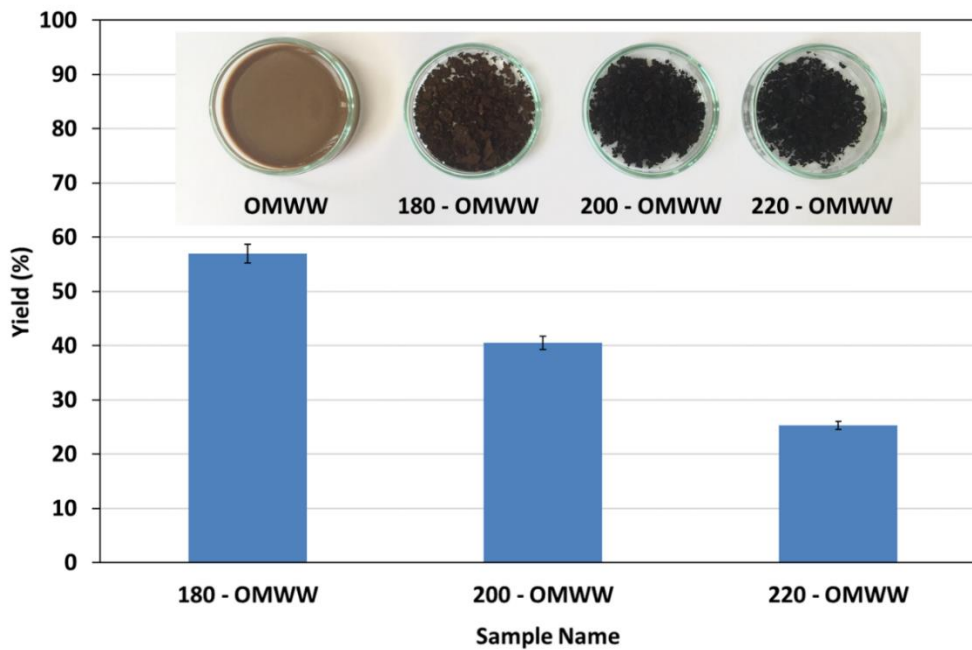
Figure 1: Effect of the used HTC temperature on the hydrochar production yields from OMWW hydrothermal carbonization at different temperatures

In order to get more information about the degradation mechanism, the thermal behavior of

the $OMWW_{SF}$ as well as the produced hydrochars was examined under inert atmosphere. Figure

2 shows three differentiable thermal degradation zones. The first mass loss extends between

ambient temperature and 120°C and is related to the elimination of water and light volatile

matter. The second and third zones were ranged between 150°C and 280°C and 280°C and 600°C, respectively (Fig. 2). The DTG of the $OMWW_{SF}$ is initially characterized by a slow decomposition rate with peak temperatures at 238°C and 320°C, then followed by a fast decomposition with a peak at 362°C (Figure 2). According to Volpe *et al.* (2018), the first two peaks are attributed to the degradation of hemicellulose and cellulose . The third peak could be attributed to an intense and fast degradation of a part of the lignin content and/or the organic soluble extractives such as alcohols and aromatic molecules (Volpe et al., 2018).

Regarding the hydrochars, it can be noticed that the broad peak at 238°C became very intense for all produced hydrochars as compared to the $OMWW_{SF}$. This could be related to the effect of heat gradient on the solid fraction leading to the defragmentation of cellulose and hemicellulose matrices into secondary chars compounds (Lucian et al., 2018). This particular aspect could be clearly observed macroscopically on the samples 200 – OMWW and 220 – OMWW characterized with a distinguishable smell and colloidal tar-like deposits.
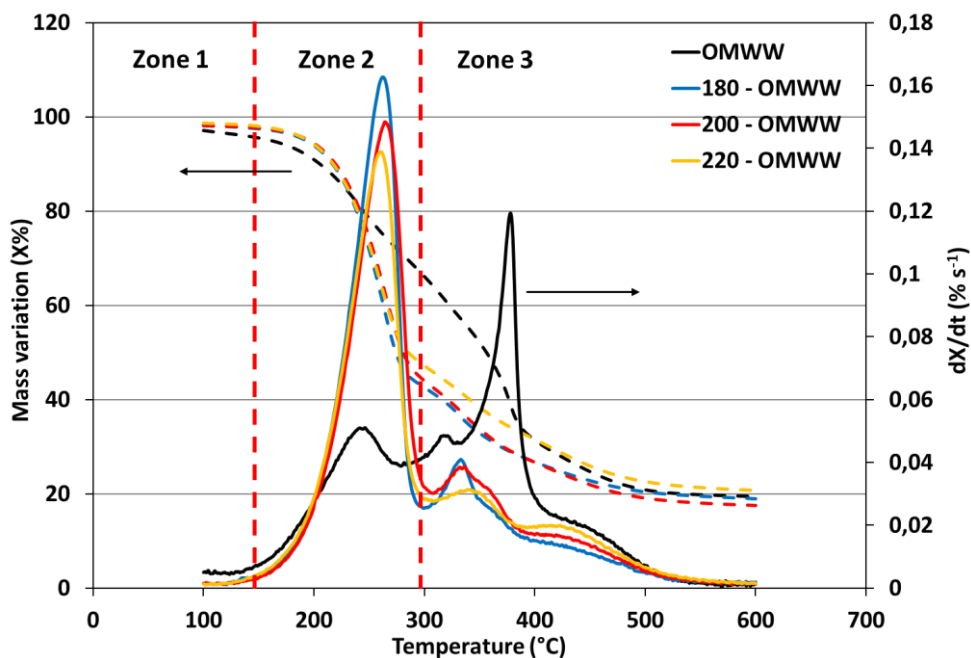
Figure 2: TGA/DTA curves under inert atmosphere of raw OMWW solid phase and the derived hydrochars at different temperatures (Full lines: DTA; Dotted lines: TGA)

On the other hand, it has been pointed out that at certain temperature and vapor pressure, aqueous media contained in the autoclave undergoes important modification at the subcritical fluid phase (Wang et al., 2018). During this time, the hydrothermal carbonization of the OMWW is submitted to a succession of reactions leading to the modification of the physico-chemical properties towards a more stable carbon material (Kruse and Dahmen, 2018). This reaction is further amplified when the media reacts as a polar organic reactant in the presence of organic compounds such as formic and acetic acids, characterizing the OMWW effluent (Atallah et al., 2019).

It is important to underline that the degradation and transformation reaction during the HTC process progress could lead to two possible outcomes: (i) dissolution of the organic and mineral matrix of the lignocellulosic material into surrounding liquid media (Poerschmann et al., 2013b) or (ii) carbon condensation reaction driven by recombination of by-products (Lin et al., 2016). Indeed, Poerschmann *et al.* (2013b) suggested that the reduction in the final solid yield during the carbonization of biomasses could lead to the migration, and thus, the increase of the dissolved organic matter in the liquid fraction. In our case, the chemical oxygen demand (COD; g O_2/L) of the raw OMWW has significantly decreased from 104 g/L to about 59 and 47 g/L for the residual liquids corresponding to the HTC of the OMWW at temperatures of 180°C to 220°C, respectively (Figure S1). This implies that during the HTC of the OMWW, the organic content in the OMWW was not modified towards the dissolution of the macropolymers constituting its lignocellulosic matrices despite the important decrease in final solid yields. Such results indicate that there was no release of organic compounds from the OMWW solid phase to the liquid fraction during the HTC process in contrast with the Poerschmann *et al.* (2013b) hypothesis,.

3.2. OMWW$_{SF}$ and hydrochars physico-chemical properties

3.2.1. Proximate and ultimate analyses

Proximate analysis of OMWW$_{SF}$ and hydrochars at different HTC temperatures aim to assess their qualityin terms of macro composition and calorific capacity. The related results (Figure 3) reveal that the OMWW$_{SF}$ contains significant percentage of volatile matter of 84% and low concentrations in fixed carbon and ash. After the HTC, the hydrochars volatile matter contents have slightly decreased reaching a value of 78.21% at 220°C. At the contrary, the hydrochars fixed carbon contents have decreased with the increase of HTC temperature. Indeed, compared to the OMWW$_{SF}$, the fixed carbon contents of the hydrochars at 180, 200 and 220°C have increased by about 6%, 10% and 14%, respectively. This outcome suggests the occurring of possible polymerization/recombination reactions with the HTC temperature increase. On the other hand, a net decrease of the ash contents was observed with temperature since it passes from 10% in the OMWW$_{SF}$ to 3% for the hydrochar produced at 220°C. This decrease could be attributed to the minerals leaching from the solid matrix to the aqueous solution, driven by heating gradient and reactivity with molecules present in the solution. Similar findings were enunciated by Volpe *et al.* (2018) when performing the HTC on Italian olive mill waste at different temperatures. Related results suggested a significant increase of fixed carbon from 20% to 26.6% and a decrease of both volatile matter from 77.9% to 70.6% and ash from 2.1% to 1.7% for raw feedstock and hydrochars produced at 220°C, respectively.
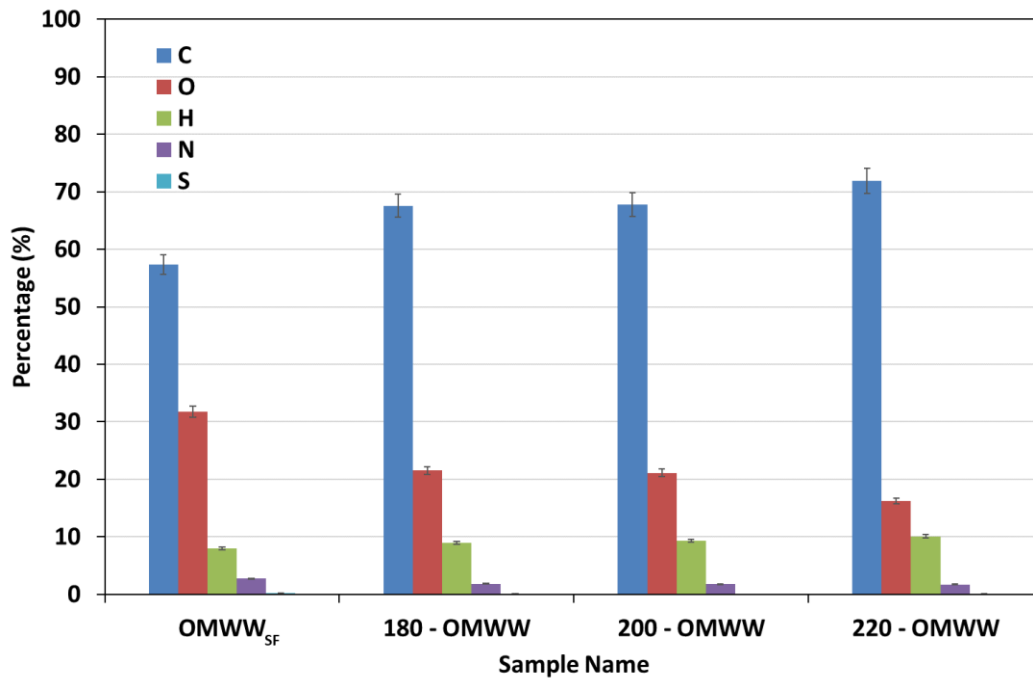
1
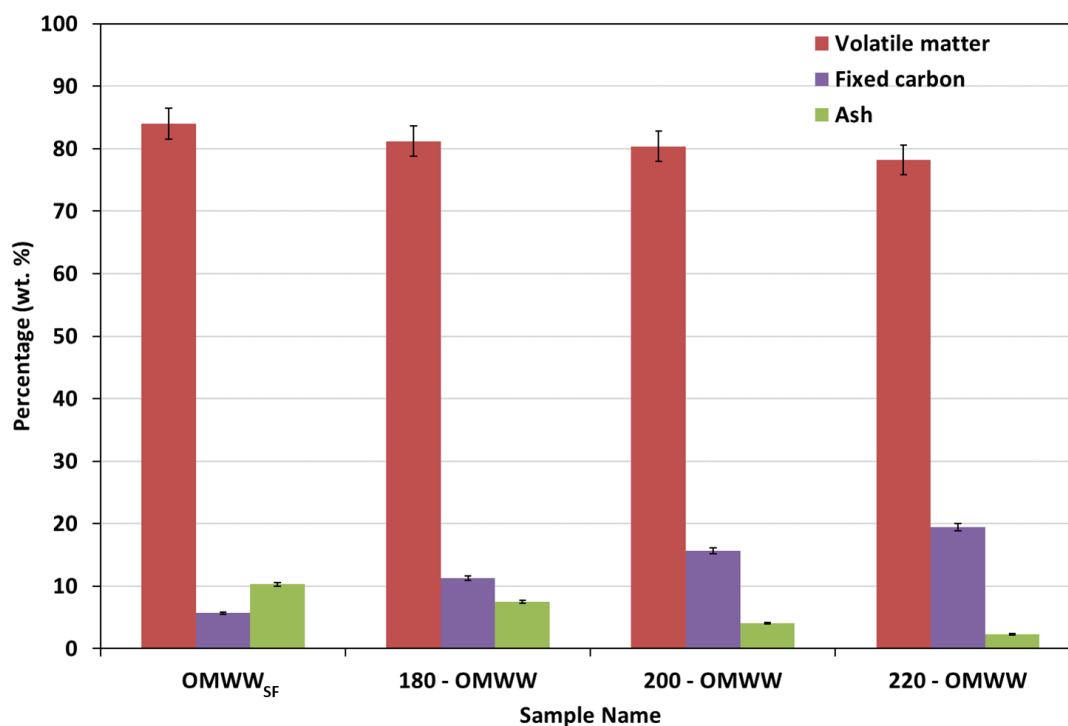
Figure 3: Proximate analysis (wt. %) of the OMWW solid fraction (OMWW$_{SF}$) and the

derived hydrochars produced from raw OMWW at 180°C, 200°C and 220°C

The CHONS composition of the OMWW$_{SF}$ and the derived hydrochars at different

temperatures is presented in Figure 4. It appears that hydrochars elemental composition was

very dependent on the HTC temperature. For instance, the OMWW$_{SF}$ carbon content has

increased from an initial 57.3% to 67.6%, 67.8% and 71.9% after HTC at 180°C, 200°C and

220°C, respectively. This finding could be imputed to a possible combination of dehydration

and decarboxylation reactions that are evidenced by the significant increase of hydrogen

contents (Figure 4). This increase could be attributed to the re-condensation of volatile matter

and organic contents present in OMWW into a more stable carbon. On the other hand, the

oxygen, nitrogen and sulfur percentages in the produced hydrochars decreased when increasing

temperatures. On the other hand, the notable decrease in the atomic ratios O/C (60% between

OMWW and 220 – OMWW) along with relatively constant H/C ratios, suggests that: i) the

degradation of the OMWW is mainly favored with a decarboxylation reaction where oxygen

1 was released in form of CO_2 gas, ii) the hydrogenic compounds were less affected by the HTC

2 temperature variations (Saqib et al., 2018). These results were found to be in concordance with

3 study conducted by Volpe *et al.* (2018) where carbon and hydrogen contents increased from

4 54.3% to 64.2% and from 6.2% to 6.6% while oxygen percentage decreased from 36.5% to

5 25.3% for $OMWW_{SF}$ and derived hydrochar produced at 220°C, respectively.

7 **Figure 4:** Elemental composition (wt. %) of the OMWW solid fraction ($OMWW_{SF}$) and the

8 derived hydrochars produced from raw OMWW at 180°C, 200°C and 220°C

9 **3.2.2. Energy content**

10 The dried $OMWW_{SF}$ is characterized with a significant HHV (26.81 MJ/kg; LHV: 25.01

11 MJ/kg) that is higher than the one observed for coal (22 MJ/kg (Saqib et al., 2018)) and similar

12 to lignite (24 MJ/kg) (Seyedsadr et al., 2018).For all produced hydrochars, the HHV increased

13 from 31.53 MJ/kg to 35.70 MJ/kg with the increase of the used HTC temperature from 180 to

14 220°C (Figure S2). Similar findings were observed for feedstocks classified between high-

15 volatile bituminous and low-rank coals which emphasizes on their possible use in energetic

16

applications (Ul Saqib et al., 2019). This outcome is related to the decrease in the O/C ratio due to the deoxygenation process during the dehydration reaction (Figure S2). On the other hand, the increase in the carbonization temperature engenders an increase in the degradation rate of the cellulose and hemicellulose into higher concentrations of intermediate by-products such as soluble aldehydes, aldols and fatty acids as well as volatile matters including alkanes (Atallah et al., 2019). These by-products, eventually incorporated in the generated solids, are usually characterized with higher calorific properties than cellulose and hemicellulose, which enhances the overall HHV of the hydrochars (Krysanova et al., 2019).

3.2.3. Morphological and structural properties of hydrochars

The SEM images of the $OMWW_{SF}$ in comparison with hydrochars show that the former solid matrix presents an heterogeneous surface with small embedded and deformed particles and the absence of any lignocellulosic developed porous structure as could be seen in wood morphology (Figure 5). After the HTC process, a significant change in the hydrochars structure could be noted. In fact, all these samples exhibited an irregular morphology consisting of microsphere aggregates with various diameters (Figure 5). Similar results were reported by Sevilla and Fuertes (2009) when studying the cellulose hydrothermal carbonization at different temperatures. Under high inner pressure and temperatures, cellulose and hemicellulose endure a condensation in the carbon content accompanied with a shifting in the crystalline arrangement, which leads to the formation of these carbon micro-spheres. According to Li *et al.* (2011), these spheres consist of small groups of fused benzene rings that form hydrophobic stable core with oxygen in the ring such as ether and pyrone molecules, while the shell presented reactive oxygen hydrophilic functionalities.
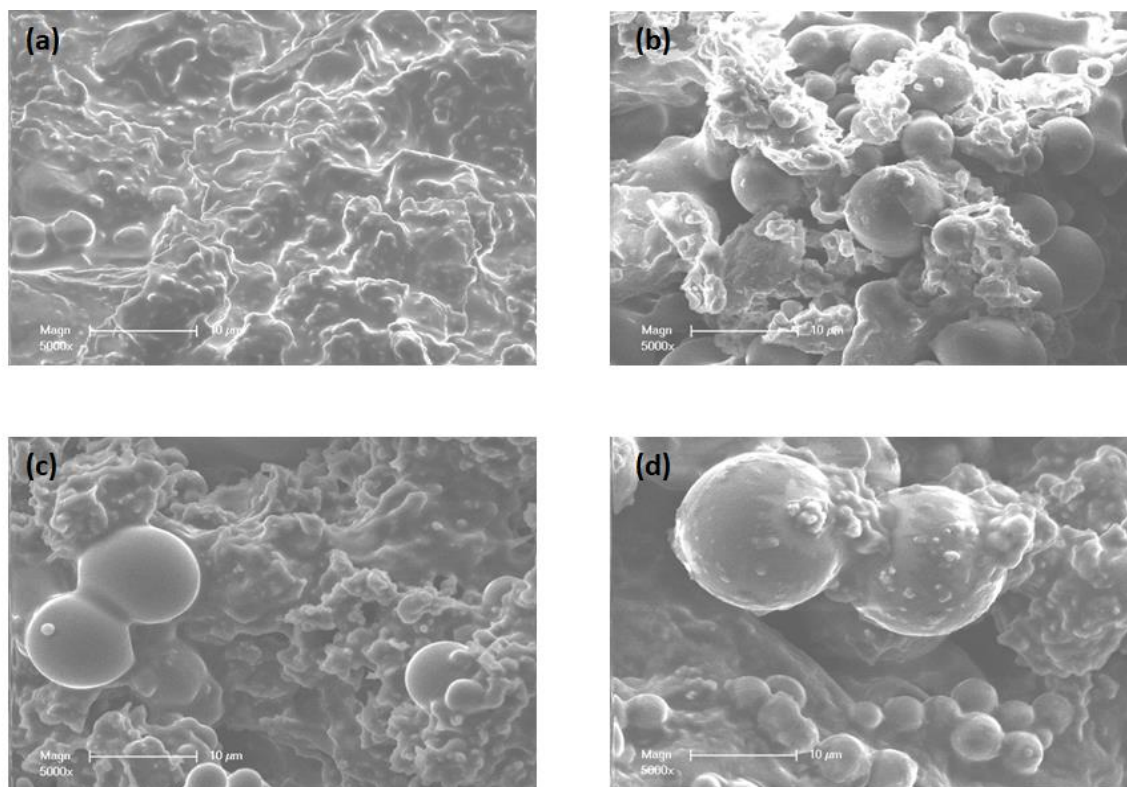
Figure 5: SEM images of the OMWW solid fraction ($OMWW_{SF}$) (a) and the produced hydrochars: at 180°C (b); 200°C (c) and 220°C (d).

On the other hand, the EDX analysis of the $OMWW_{SF}$ revealed a highly uniform dispersion of carbon and oxygen (Figure S3). Moreover, the EDX cartographies showed a notable presence of potassium along with a homogeneous partition of minerals namely, sodium, magnesium, sulfur and chlorine (Figure S3.a – d, Table S2). After HTC, the oxygen partition decreased noticeably with increasing temperature (Table S2). Although the minerals presented a rather uniform dispersion in the samples, their contents followed the same trend with the disappearance of sodium and calcium at 200°C and 220°C (Figure S3.c). It is worth highlighting that for the sample 180 – OMWW, a certain singularity was remarked where a conglomeration-like spot is mainly composed of oxygen and calcium, revealing their possible crystallization in the form of calcite.

18

In order to understand the effect of the HTC temperature on the hydrochars structural properties, XRD patterns of raw and carbonized solid materials were carried out (Figure S4). The related diffractograms emphasize on the heterogeneous hydrochars aspect including both crystalline (mainly inorganic impurities) and amorphous-like organic molecules (cellulose, lignin and extractives) structural patterns. Firstly, a characteristic wide peak at 21° was detected for the OMWW$_{SF}$ representing the amorphous cellulose phase (Guo et al., 2015). This peak was also detected for the hydrochars produced at different temperatures suggesting that no specific structural rearrangement of cellulose was established during the hydrothermal carbonization. The XRD showed also sharp peaks attributed to the quartz (SiO$_2$; COD 4115457), calcium oxalate (CaC$_2$O$_4$; COD 9000827), calcite (CaCO$_3$; COD 1010928; COD 1010962) and potassium chloride (KCl; COD 1000050) structures (Khiari et al., 2019). It could be noted that potassium was present in the form of KCl crystalline structure in feedstock then became more abundant after hydrothermal carbonization, especially at 200°C. It is also remarkable that peaks at 32.2° and 36.2° indicating the presence of CaCO$_3$ in the OMWW$_{SF}$ were identified after hydrothermal carbonization as calcium oxalate and calcium phosphate (CaC$_2$O$_4$; Ca$_3$(PO$_4$)$_2$; COD 2106194; COD 1517238) crystallographic structures (Figure S4). This transformation could be attributed to a decomposition reaction of calcium carbonate in the presence of acids in the liquid phase, leading to the precipitation of calcium oxalate and calcium phosphate and the liberation of H$_2$O molecules. Although the mineral quantification (Section 3.2.4) suggests the decrease in phosphorus and potassium (Table 1, Table S2), it is possible that the increase in carbonization temperature contributed to the fixation of P and K in a more stable form, especially in the presence of calcium and chloride ions (Cui et al., 2020).

3.2.4. Mineral composition of hydrochars

The nutrient elements contents represent a very interesting feature of hydrochars to determine their possible applicability in the agricultural field. Table 1 show that the OMWW$_{SF}$

is characterized with an important concentration of minerals, with a total soluble NPK content of 63.6 g/Kg. With increasing the used HTC temperature, this amount decreased significantly by about 57%, 82% and 87% for treatment operated at 180°C, 200°C and 220°C, respectively (Table 1). This finding is in opposition to what was reported in literature. In fact, an increasing in the HTC temperature of lignocellulosic material in distilled water and collected sewage sludge favored the immobilization of the nutrients inside the final hydrochar during the recombination reaction (Chen et al., 2017; Ovsyannikova et al., 2019). The recorded decrease in present study could be related to the nature of the specific liquid media and its composition (OMWW). In fact, liquid media severity could significantly enhance the acidification of the hydrochars and thereby the minerals release from the solid fraction to the liquid one (Huang et al., 2019). Moreover, it is remarked that the percentage of the total soluble N has decreased by increasing carbonization temperature from 17600 mg/kg to 6430 mg/kg (Table 1). Despite the decreasing trend, the content in nitrogen is considered to be high compared to other minerals. Moreover, compared to slow pyrolysis, the nitrogen is advantageously incorporated to a certain extent in the hydrochars (Haddad et al. 2017). It is possible that during carbonization, amino compounds and cellulose degradation by-products endured a Maillard reaction, characterized with the polymerization of aldehydes and aldols with amino compounds to obtain polymers with high nitrogenous content (Chen et al., 2017; Wang et al., 2018).

Table 1: Mineral composition (wt. %) of the OMWW solid fraction (OMWW$_{SF}$) the and the produced hydrochars from the HTC of raw OMWW at 180°C, 200°C and 220°C.

	Potassium (mg/kg)	Sodium (mg/kg)	Calcium (mg/kg)	Magnesium (mg/kg)	Phosphorus (mg/kg)	Total Nitrogen (mg/kg)	Ammoniacal Nitrogen (NH$_4$-N; mg/kg)
OMWW$_{SF}$	44000	3700	1421	1744	2034	17600	14.2
180 - OMWW	20000	1840	62.2	503	618	6760	4.71
200 - OMWW	3350	256	3.50	23.9	66.7	8220	0.00
220 - OMWW	2000	172	6.60	8.7	34.8	6430	0.00

3.3. Mineral and organic composition of liquid fractions

3.3.1. Mineral composition

To establish a global overview about the fate of minerals, the content of five minerals, namely potassium, sodium, calcium, magnesium and phosphorus in the residual liquid fraction was measured after HTC process and results were depicted in the Table S3.

It appears that the raw OMWW liquid fraction possesses relatively high concentrations of alkaline earth and alkali metals, especially potassium where its concentration was higher than 5.1 g/L. After the HTC, it could be clearly remarked that the minerals, even presenting similar

valence, could behave differently at increasing temperature. For example, the potassium contents in the liquid fraction is almost constant after treatments at 180°C, 200°C and 220°C, respectively. In this context, Xiong *et al.* (2019) studied the hydrothermal carbonization of swine manure at different temperatures. They report, a rather constant content of soluble potassium concentrations, varying between 1462.2 mg/L and 1405.2 mg/L for carbonization at 200°C and 280°C, respectively. On the other hand, sodium content in the OMWW liquid fraction decreased by about 15%, 48% and 19% after its HTC at temperatures of 180, 200 and 220°C, respectively. It has been reported that potassium and sodium concentrations are usually characterized with similar tendency during hydrothermal carbonization as they have a high affinity to liquid fraction (Wang et al., 2019). Nevertheless, the results do not show any remarkable increase in the liquid concentration of these two alkali ions (Table 1 and Table S3). Calcium and magnesium content in liquid fraction followed the same trend during HTC (Table S3). In fact, both contents of Ca^{2+} and Mg^{2+} ions remained approximately constants in the range of 42.9-44.0 mg/L and 124.5-131.1 mg/L, respectively.

However, phosphorus content in the liquid fraction, presented a significant decrease with increasing carbonization process. The concentration in liquid fraction went from 1.66 mg/L to 0.37 mg/L for OMWW and 220 – OMWW, respectively. The increase in media severity is function of carbonization time and temperature. The intense modifications endured by water under subcritical conditions during HTC engenders its auto-ionization and the formation of acidic hydronium ions (Wang et al., 2019). At low pH values, these ions cause the hydrolysis of cellulose and hemicellulose matrices and thereby the liberation of inorganics in the liquid fraction. Subsequently, a possible diffusion of positively charged ions/molecules into hydrochars solid matrix could trigger a cation exchange reaction with soluble phosphorus, then in lower degree, Na^+, K^+, Ca^{2+} and Mg^{2+} ions, respectively, into more soluble crystalline

structures. These results are in agreement with the proximate analysis where carbonization at higher temperatures and at low pH medias is favorable for the ash leaching (Figure 3).

3.3.2. Organic composition

GC-MS analysis allowed the identification of a large number of compounds present in the raw and carbonized OMWW fractions. Table S4 shows the main detected compounds, their assignments and retention times. Notably, liquid fractions were characterized with high contents in some sugar alcohol derivatives like glycerol, sorbitol and myoinositol, different acid compounds (succinic acid, quinic acid and pyroglutamic acid, the latter being an amino acid derivative) as well as two compounds found in abundance in olive, namely tyrosol and hydroxytyrosol.

It has been remarked that HTC impacted identically on certain family of compounds. A prominent increase of some amino acids was noted in particular between 180°C and 200°C, such as glycine, alanine, valine, isoleucine, leucine and proline. All these amino acids possess a neutral and hydrophobic side chains with the exception of pyroglutamic acid. The opposite behavior was noted for sugars and sugar derivatives, with a decrease or even the disappearance of monosaccharides, disaccharides and monosaccharide acids (Table S4). On the other hand, monosaccharides alcohol was not affected by HTC with the exception of glycerol and sorbitol concentrations which increased after carbonization process. Finally, a reduction of free fatty acids like palmitic and stearic acids is noted.

Despite the major differences concerning the derivatization procedure and the sampling methodology during GC-MS analysis, considerable resemblances could be reported in some related references. For instance, in the study conducted by Poerschmann *et al.* (2013a) on the OMWW hydrothermal carbonization, the use of different temperature gradients (from 40°C to 260°C or 310°C depending on the column type), allowed the detection of low boiling point

compounds in particular formic and acetic acids, methanol and ethanol. Authors also reported the presence of glucitol and inositols at important concentrations along with the annotation of two dipyrrolo-pyrazine molecules obtained by a cyclization of amino acids (Poerschmann et al., 2013a). In this study, the applied gradient of temperature ranged between 110°C to 350°C allowed the identification of few mono- and disaccharides (Table S4). Nevertheless, various numbers of similar abundant molecules were detected such as tyrosol and hydroxytyrosol, malonic and succinic acids and glycerol (Poerschmann et al., 2013a).

Moreover, concerning sugar derivatives, sorbitol is the most abundant sugar alcohol with another C6-sugar alcohol, galactitol, and three inositol isomers including two well-identified, scyllo-inositol and myo-inositol were found (Table S4). Finally, two dipyrrolo-pyrazine molecules obtained by a cyclization of amino acids were annotated in the literature (Poerschmann et al., 2013a). This type of products, namely 2,7-dihydroxyoctahydro-5h,10h-dipyrrolo[1,2-a:1',2'-d]pyrazine-5,10-dione were obtained in this work. These type of molecules were obtained by intermolecular condensation of two amino acids by dehydration during pyrolysis (Chiavari and Galletti, 1992; Ratcliff et al., 1974). Similar results were also stated in the investigation of Poerschmann *et al.* (2013b) dealing with the hydrothermal carbonization of OMWW at different temperatures. Reported findings suggested a global increase in the quantity of sugar alcohol and equivalent concentration for tyrosol and hydroxytyrosol with a decrease in the free fatty acids' concentrations (palmitic and stearic acids).

For all applied temperatures during HTC, the organic profile of T-OMWW liquid samples are very similar. Some compounds, however, were clearly impacted such as penta-1,2,5-triol and 2-methylsuccinic acid whose contents increased with increasing the HTC temperatures. On the other hand, the content in other compounds were found to decrease at high temperature. In fact, the contents of all natural amino-acids decreased significantly at higher HTC temperature

as well as the free fatty acids (palmitic and stearic), certain organic acids (like malic, maleic, methylmaleic,3-hydroxy-3-methylglutaric, 2-furoic and itaconic acid) and few monosaccharide alcohol (such as arabitol, threitol) and the C5-sugar (Table S4).

It is interesting to note that few molecules with agronomic interest could be identified among the abundant compounds present in different T-OMWW samples (Figure S5, 180-OMWW). For instance, sugar alcohols like sorbitol, galactitol, myo-inositol and glycerol are particularly known for their role in mitigating biotic and abiotic stress factors threatening crop development as well as their common use as osmoprotectants (Kanayama, 2009; R.K. Sairam et al., 2006). Theerakulpisut and Gunnula showed also that an exogenous supply of sorbitol seems to have a protective role in case of an osmotic stress for salt-sensitive plants (Theerakulpisut and Gunnula, 2012). Furthermore, glycerol was found to stimulate the growth of various crops and regulate plant disease resistance against bacterial pathogens (Qian et al., 2015; Tisserat and Stuff, 2011). Myo-inositol, on the other hand, has the ability to prevent against the negative effects of drought or salinity stresses such as Reactive Oxygen Species accumulation (Hu et al., 2018; Yildizli et al., 2018). Concerning amino and pyroglutamic acids they present the capacity to counteract an osmotic imbalance and reduce the impact of water deficit by increasing crop yield (Jiménez-Arias et al., 2019).

3.4. Surface chemistry of hydrochars

The impact of the hydrothermal carbonization of OMWW on the hydrochars surface properties was assessed by three complementary techniques, namely surface functional groups identification and quantification by IR spectroscopy, Boehm titration method and pH at neutral surface charge (pH_{ZPC}) (Figures 6 and 7). The infrared spectra of hydrochars issued from OMWW carbonization are presented in Figure 6. The FTIR analysis presented a large number

1 of peaks that emphasized on the heterogeneous structure of the hydrochar's surface, with the

2 presence of several functional groups.
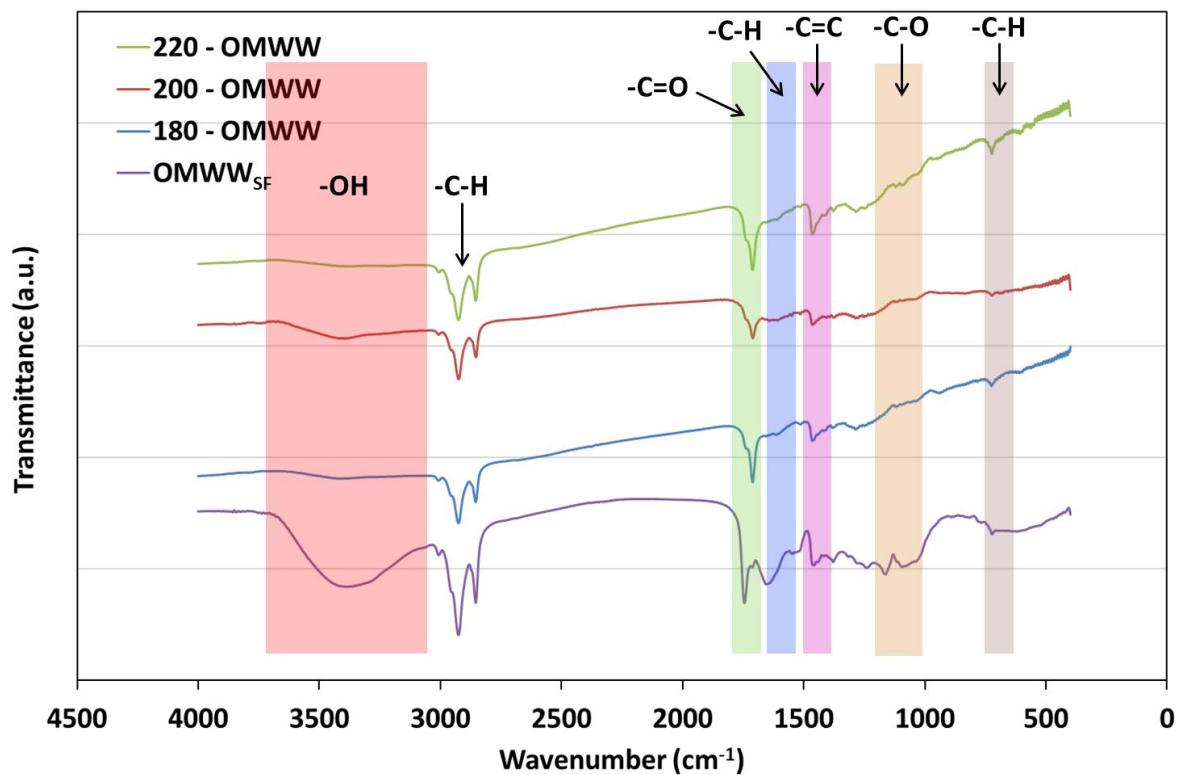
4 **Figure 6:** FTIR specters for the raw OMWW solid fraction (OMWW$_{SF}$) and the derived

5 hydrochars produced from raw OMWW at 180°C, 200°C and 220°C

6   The broad peak detected between 4000 cm^{-1} and 3300 cm^{-1} corresponds to O-H groups

7 related to the stretching of hydroxyl and carboxyl functional groups. This peak constantly

8 decreased in intensity and wavenumber while increasing carbonization temperature. This could

9 be attributed to the increase in carbon content in the hydrochar associated with a decrease in

10 the oxygen percentages driven mainly by a decarboxylation/polymerization reactions (Méndez

11 et al., 2019). At 1700 cm^{-1}, we noticed a shifting in peak related to –C=O functional groups

12 with about -35 cm^{-1}, between OMWW and 180 – OMWW. Afterwards, the peak remained

13 constant when further increasing the temperature. This observation could be attributed to the

14 involvement of carbonyl, ester and carboxylic groups of the lignin structure during

carbonization reaction (Guo et al., 2015). On the other hand, two peaks detected for the OMWW

specter at 1624 cm^{-1} and 1598 cm^{-1} related to C=C groups have almost disappeared for all the

hydrochars samples. This behavior suggests the absence of any detectable stretches of the lignin

aromatic skeletal structure even at low carbonization temperatures, which is in concordance

with the previous TGA results (Figure 2). This is further confirmed by the peak of the C–O

bonds detected between 1114 cm^{-1} and 1045 cm^{-1} only for OMWW corresponding to the

vibrations in lignin structure, which disappeared after carbonization (Figure 6). On the other

hand, peaks detected at 2922 cm^{-1} and 721 cm^{-1} related to the aliphatic C-H stretches and

aromatic –C-H bands, respectively, remained fairly unmodified.

These results were further confirmed when quantifying the surface functional groups

through Boehm titration (Figure 7). The identification of three different acidic functional groups

namely phenolic, carboxylic and lactonic was achieved. The OMWW solid fraction is

characterized by an important content of total functional groups (1155 µmol/g), with a high

content in carboxylic and phenolic functional groups (494.21 and 654.59 µmol/g, respectively)

and low concentration of lactonic groups (6.40 µmol/g) (Figure 7). After HTC at 180°C, the

carboxylic and phenolic groups decreased to only 27.48 µmol/g and 148.22 µmol/g. As

treatment temperatures increases, a quasi-disappearance of phenolic groups was noted at 220°C

with an estimated concentration of 12.16 µmol/g. On the other hand, with the increase of the

HTC temperature, a gradual increase in the carboxylic and lactonic groups' concentrations was

remarked until reaching 374.5 and 94.5 µmol/g, respectively, for the sample 220 – OMWW

(Figure 7). This observation could be attributed to the media status during the hydrothermal

carbonization. At relatively lower temperatures, it seems that heat diffusion rate was more

important, which enhanced the dehydration reaction and the release of hydrogen from

carboxylic ($–COO^- + H^+$) and phenolic ($R –CO^- + H^+$) groups in the form of H_2O. This is in in

line with the found atomic H/C ratios showing the lowest value at 180°C (Table 1). On another

hand, the increase in lactonic groups could be attributed to the involvement of these groups in the formation of the spherical carbon nanoparticles. Nevertheless, this difference in trends between functional groups was explained by the fact that auxiliary and antagonist reactions are susceptible to undergo during the hydrothermal carbonization of OMWW (Saha et al., 2019).

Regarding the final pH of the residual liquid phases, as well as the pH_{ZPC} of the generated hydrochars, it appears that OMWW presents an acid aspect with a pH value of 4.68 which lays in the range of pH reported in previous papers (Galiatsatou et al., 2002; Poerschmann et al., 2013b). The general trend after carbonization suggests a slight increase of the final pH, from 5.01 to 5.79. It has been reported that OMWW contains high concentrations of polyphenolic compounds and fatty acids that could intervene in the carbonization mechanism (Poerschmann et al., 2013a). These compounds are susceptible to react with OH^- functional groups present on the OMWW's solid fraction either by neutralizing them or by reducing them towards the liquid phase (Saha et al., 2019). Another possible mechanism could be related to the important synthesis of ammonia alkaline groups by the successive degradation of amino acids (Wang et al., 2019). These findings where further confirmed when analyzing the pH_{ZPC} values of the biomasses and the produced hydrochars (Figure 7). In fact, while increasing carbonization temperature from 180°C to 220°C, pH_{ZPC} decreased from 3.16 to 2.48. This could be explained by the fact that the carbonization mechanism tends toward the isomerization of glucose molecules of the cellulose and hemicellulose matrices for the production of long chained organic acids such as lactic, formic and luvulinic acids (Li et al., 2015). The rearrangement of these chains is intensified when using the OMWW as acidic carbonization media which led to hydrochars with lower surface pH. It could be interesting therefore to investigate the potential application of such hydrochars chars issued from the HTC of OMWW for the amendment of alkaline and sub-alkaline soils for the cultivation of nitrogen

1 fixing/tolerant crops such as fenugreek and soybeans (Baghbani-Arani et al., 2017; Landriscini

2 et al., 2019).
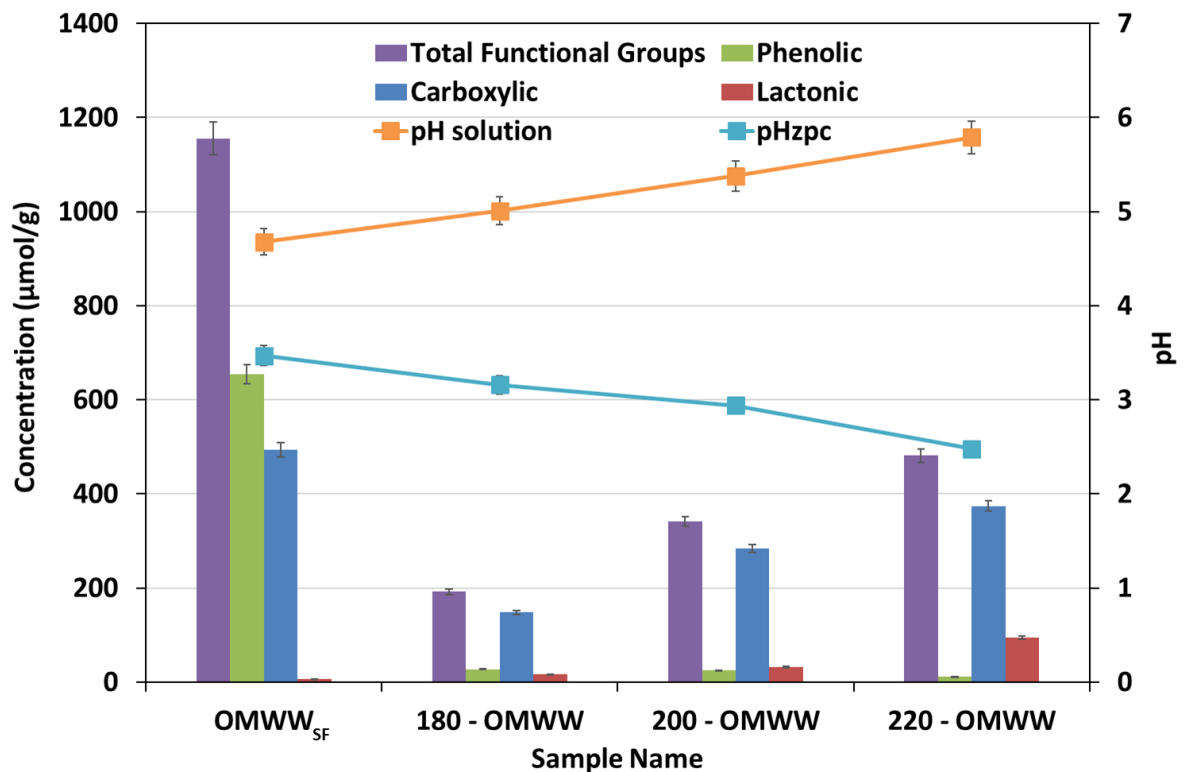
3

4 **Figure 7:** Acidic functional groups concentration (µmol/g), final solution pH and surface pH

5 at zero-point charge (pH$_{ZPC}$) of the raw OMWW solid fraction (OMWW$_{SF}$) and the produced

6 hydrochars from the HTC of OMWW at 180°C, 200°C, and 220°C

4. Discussions

4.1. Mechanism of the OMWW Hydrothermal Carbonization

9   The HTC was found to be very useful to directly convert the OMWW into hydrochars

10 without using supplementary clean water source. Such treatment performed at different

11 carbonizations temperatures had important impacts on the derived hydrochar properties. The

12 morphology, the surface chemistry and the structure have been modified. HTC of biomasses

13 leads to the formation of a primary char, i.e. hydrochar in addition to media by-products namely

14 bio-oil and a carbonization gas. At extended carbonization periods with high inner pressure and

temperatures, the early stage degradation by-products contribute to the increase of the liquid media severity. In such favorable conditions, it has been reported that the solubilized molecules, especially alcohols, mono- and polyphenols undergo a polymerization reaction, characterized with a reduction in the total organic carbon (TOC) content present in the final process water, the production of syngas (light hydrocarbons, hydrogen and carbon oxides) and along with significant amount of tarry condensate (Gai et al., 2016; García-Jarana et al., 2014). In a recent study, Duman *et al.* (2018), studied the carbonization of food waste for the production of syngas (H_2 and CH_4). They pointed out that the addition of alkali catalyst, i.e., K_2CO_3, increased in the subcritical water basicity which enhanced the formation of low molecular weight compounds. Consequently, the increase in intermediate organics concentration enhanced hydrogen and methane yields as well as the formation of tar as a non-desirable by-product.

Another mechanism worth highlighting is the obtention of spherical particles as result of the condensation of aromatic skeletal into simpler and more stable sugars, namely cellulose then glucose. According to LaMer reaction (Lamer and Dinegar, 1950), it is possible that the subcritical conditions occurring during the HTC led to the aggregation of the soluble polymers and their degradation by-products on the solid's surface followed by their rearrangement in the form of carbon nanospheres. Although the materials contain carbon as major component (up to 71.9% for 220 – OMWW) they are characterized also by high amounts of inorganics and heteroatoms (N, P and K). The inorganics (Ca^{2+}, Cl^-…) are crystalline in nature as shown by XRD. Such compounds were found to diminish after the HTC as emphasized by solid extraction and EDX techniques, which could be associated to a leaching reaction in the liquid media. Although this can be seen as an inconvenient for the solid hydrochar, such by-product liquid which is acidic can be used as fertilizer for alkaline soils. On the other hands, the reactions (polymerizations, decarboxylations…) occurring during the HTC may also be responsible for such behavior. Finally, the energetic properties were found to be interesting as they raise the

recovered hydrochar's HHV from a sub-bituminous to low-rank coal. This finding was demonstrated by the correlation between the decrease in the O/C ratio and the increase of the HHV of the hydrochars. This opens the door for the possible use of these materials in energetic applications and the reduction of the oxygen content by controlling the carbonization atmosphere.

4.2. Properties and Potential Applications

Hydrochars resulting from the HTC of OMWW present a very low content in alkaline and alkaline earth metals (AAEMs) (K^+, Na^+, Ca^{2+} and Mg^{2+}) and a high content in pnictogens (Total P and N). After HTC, the content in nitrogen remained relatively high. The concentration of these minerals in the final solid could determine the proper use of hydrochars in the suitable economical field. In fact, the increase in the HHV of the produced hydrochars is not only in correlation with the decreasing O/C atomic ratio (Figure S2), but is also function of the reduced content in minerals. Multiple studies used hydrothermal carbonization as a solution for the removal of minerals from hydrochars at modified low pH media prior a thermal carbonization (over 900°C) in the aim of producing a clean solid fuel (Huang et al., 2019; Zhao et al., 2020). To overcome this decrease, controlled impregnation of the lacking minerals after hydrothermal carbonization could be envisaged.

As mentioned, the HTC of OMWW resulted in hydrochars with important final content in nitrogen. Such outcome is not possible when employing conventional thermal treatment methods such as slow pyrolysis. In fact, biochars issued from pyrolysis are characterized with an alkaline pH, high content in carbon and very low concentrations in nitrogen (Ibn Ferjani et al., 2019). Therefore, a complementary method that consists of soil amendment by mixtures of hydrochars/biochars could be envisaged for an optimal carbon sequestration and to ensure the bioavailability of N, P and K elements.

On the other hand, a special attention is highly recommended for the valorization of the liquid fraction issued from the HTC. Indeed, it is rich in acids, sugar derivatives and nutrients that could be very beneficial for plants growth. This liquid phase could be appropriately treated by various hybrid technologies in order to be in conformity with the fixed norms for wastewaters reuse in agriculture (Benavente et al., 2017). Improvements of this liquid phase quality should mainly concern its aqueous pH, electrical conductivity or salinity and chemical oxygen demand (or organic matter content). On the other hand, the contained nutrients could be extracted through their enhanced precipitation as struvite for a further subsequent use in agriculture as slow release biofertilizer (Chu et al., 2020).

5. Conclusions

Hydrothermal carbonization was successfully applied for the OMWW conversion into a carbon-rich material. The hydrochar production yield was found to decrease with increasing temperature and understood mainly by the degradation of the lignocellulosic matrix. Accordingly, the increase in temperature resulted in a three folds enhancement of the fixed carbon content, which was accompanied by a decrease in the ash and volatile matter percentages. These results were further confirmed by ultimate analysis, emphasizing on the condensation of carbon content and the reduction of volatile matter and ash percentages. The reduction in the O/C atomic ratio and the decrease in the inorganics' presence allowed the synthesis of hydrochars with promising energy contents up to HHV of 35.70 MJ/kg for 220 – OMWW. Moreover, the heat intake modified severely the surface morphology of the hydrochars, with the appearance of carbon microspheres related to the degradation of lignocellulosic matrix and the recombination of the resulting by-product into hydrophilic aromatic structures. Such morphological aspect could be of significant importance to increase diffusion in case of application in the energetic field and agriculture considering their well shaped form. The liquid fraction composition was quantified and presented high concentrations

32

in acids, phenols and sugar derivatives which varies with temperature. These by-products are commonly used to protect crops from stressful environments as efficient regulators for osmose phenomenon in case of water drought and soils with high salinity.

Acknowledgments

References

Aktas, E.S., Imre, S., Ersoy, L., 2001. Characterization and lime treatment of olive mill wastewater. Water Res. https://doi.org/10.1016/S0043-1354(00)00490-5

Allan Moore, W., Kroner, R.C., Ruchhoft, C.C., 1949. Dichromate Reflux Method for Determination of Oxygen Consumed. Anal. Chem. https://doi.org/10.1021/ac60032a020

Atallah, E., Kwapinski, W., Ahmad, M.N., Leahy, J.J., Al-Muhtaseb, A.H., Zeaiter, J., 2019. Hydrothermal carbonization of olive mill wastewater: Liquid phase product analysis. J. Environ. Chem. Eng. https://doi.org/10.1016/j.jece.2018.102833

Azzaz, A.A., Jellali, S., Assadi, A.A., Bousselmi, L., 2015. Chemical treatment of orange tree sawdust for a cationic dye enhancement removal from aqueous solutions: kinetic, equilibrium and thermodynamic studies. Desalin. Water Treat. 3994, 1–13. https://doi.org/10.1080/19443994.2015.1103313

Azzaz, A.A., Khiari, B., Jellali, S., Matei Ghimbeu, C., Jeguirim, M., 2020. Hydrochars

production, characterization and application for wastewater treatment: A review. Renew. Sustain. Energy Rev. Under Pres. https://doi.org/10.1016/j.rser.2020.109882

Baghbani-Arani, A., Modarres-Sanavy, S.A.M., Mashhadi-Akbar-Boojar, M., Mokhtassi-Bidgoli, A., 2017. Towards improving the agronomic performance, chlorophyll fluorescence parameters and pigments in fenugreek using zeolite and vermicompost under deficit water stress. Ind. Crops Prod. https://doi.org/10.1016/j.indcrop.2017.08.049

Bargmann, I., Rillig, M.C., Buss, W., Kruse, A., Kuecke, M., 2013. Hydrochar and biochar effects on germination of spring barley. J. Agron. Crop Sci. https://doi.org/10.1111/jac.12024

Bargmann, I., Rillig, M.C., Kruse, A., Greef, J.M., Kücke, M., 2014. Effects of hydrochar application on the dynamics of soluble nitrogen in soils and on plant availability. J. Plant Nutr. Soil Sci. https://doi.org/10.1002/jpln.201300069

Benavente, V., Fullana, A., Berge, N.D., 2017. Life cycle analysis of hydrothermal carbonization of olive mill waste: Comparison with current management approaches. J. Clean. Prod. https://doi.org/10.1016/j.jclepro.2016.11.013

Boehm, H.P., 2002. Surface oxides on carbon and their analysis: A critical assessment. Carbon N. Y. 40, 145–149. https://doi.org/10.1016/S0008-6223(01)00165-8

Chatzisymeon, E., Foteinis, S., Mantzavinos, D., Tsoutsos, T., 2013. Life cycle assessment of advanced oxidation processes for olive mill wastewater treatment. J. Clean. Prod. https://doi.org/10.1016/j.jclepro.2013.05.013

Chen, X., Lin, Q., He, R., Zhao, X., Li, G., 2017. Hydrochar production from watermelon peel by hydrothermal carbonization. Bioresour. Technol. https://doi.org/10.1016/j.biortech.2017.04.012

Chiavari, G., Galletti, G.C., 1992. Pyrolysis-gas chromatography/mass spectrometry of amino acids. J. Anal. Appl. Pyrolysis 24, 123–137. https://doi.org/10.1016/0165-2370(92)85024-F

Chouchene, A., Jeguirim, M., Favre-Reguillon, A., Trouvé, G., Le Buzit, G., Khiari, B., Zagrouba, F., 2012. Energetic valorisation of olive mill wastewater impregnated on low cost absorbent: Sawdust versus olive solid waste. Energy 39, 74–81. https://doi.org/10.1016/j.energy.2011.03.044

Chu, Q., Xue, L., Singh, B.P., Yu, S., Müller, K., Wang, H., Feng, Y., Pan, G., Zheng, X., Yang, L., 2020. Sewage sludge-derived hydrochar that inhibits ammonia volatilization, improves soil nitrogen retention and rice nitrogen utilization. Chemosphere. https://doi.org/10.1016/j.chemosphere.2019.125558

Chung, J.W., Foppen, J.W., Gerner, G., Krebs, R., Lens, P.N.L., 2015. Removal of rotavirus and adenovirus from artificial ground water using hydrochar derived from sewage sludge. J. Appl. Microbiol. https://doi.org/10.1111/jam.12863

Cui, X., Lu, M., Khan, M.B., Lai, C., Yang, X., He, Z., Chen, G., Yan, B., 2020. Hydrothermal carbonization of different wetland biomass wastes: Phosphorus reclamation and hydrochar production. Waste Manag. https://doi.org/10.1016/j.wasman.2019.10.034

Dieguez-Alonso, A., Funke, A., Anca-Couce, A., Rombolà, A.G., Ojeda, G., Bachmann, J., Behrendt, F., 2018. Towards biochar and hydrochar engineering-influence of process conditions on surface physical and chemical properties, thermal stability, nutrient availability, toxicity and wettability. Energies. https://doi.org/10.3390/en11030496

DIN, 2005. Testing of solid and liquid fuels: determination of gross calorific value by the bomb calorimeter and calculation of net calorific value. Part 3: method using adiabatic jacket

51900–3.

Donar, Y.O., Çağlar, E., Sinağ, A., 2016. Preparation and characterization of agricultural waste biomass based hydrochars. Fuel 183, 366–372. https://doi.org/10.1016/j.fuel.2016.06.108

Doula, M.K., Kavvadias, V., Elaiopoulos, K., 2013. Proposed soil indicators for olive mill waste (OMW) disposal areas. Water. Air. Soil Pollut. https://doi.org/10.1007/s11270-013-1621-2

Duman, G., Akarsu, K., Yilmazer, A., Keskin Gundogdu, T., Azbar, N., Yanik, J., 2018. Sustainable hydrogen production options from food wastes. Int. J. Hydrogen Energy. https://doi.org/10.1016/j.ijhydene.2017.12.146

Fang, J., Gao, B., Zimmerman, A.R., Ro, K.S., Chen, J., 2016. Physically (CO_2) activated hydrochars from hickory and peanut hull: Preparation, characterization, and sorption of methylene blue, lead, copper, and cadmium. RSC Adv. 6, 24906–24911. https://doi.org/10.1039/c6ra01644h

Fezzani, B., Cheikh, R. Ben, 2010. Two-phase anaerobic co-digestion of olive mill wastes in semi-continuous digesters at mesophilic temperature. Bioresour. Technol. https://doi.org/10.1016/j.biortech.2009.09.067

Food and Agriculture Organization, F., 2017. Olive and Olive oil production [WWW Document]. URL http://www.fao.org/faostat/en/#home. Mediterranean region/ Agricultural type/ Olive & Olive oil

Gai, C., Guo, Y., Liu, T., Peng, N., Liu, Z., 2016. Hydrogen-rich gas production by steam gasification of hydrochar derived from sewage sludge. Int. J. Hydrogen Energy. https://doi.org/10.1016/j.ijhydene.2015.12.188

1   Gajić, A., Ramke, H.G., Hendricks, A., Koch, H.J., 2012. Microcosm study on the

2   decomposability of hydrochars in a Cambisol. Biomass and Bioenergy.

3   https://doi.org/10.1016/j.biombioe.2012.09.036

4   Galiatsatou, P., Metaxas, M., Arapoglou, D., Kasselouri-Rigopoulou, V., 2002. Treatment of

5   olive mill waste water with activated carbons from agricultural by-products. Waste Manag.

6   https://doi.org/10.1016/S0956-053X(02)00055-7

7   García-Jarana, M.B., Sánchez-Oneto, J., Portela, J.R., Martínez de la Ossa, E.J., 2014.

8   Supercritical Water Gasification of Organic Wastes for Energy Generation, in:

9   Supercritical Fluid Technology for Energy and Environmental Applications.

10   https://doi.org/10.1016/B978-0-444-62696-7.00010-1

11   Graulis, S., Chateigner, D., Downs, R.T., Yokochi, A.F.T., Quirós, M., Lutterotti, L.,

12   Manakova, E., Butkus, J., Moeck, P., Le Bail, A., 2009. Crystallography Open Database -

13   An open-access collection of crystal structures. J. Appl. Crystallogr.

14   https://doi.org/10.1107/S0021889809016690

15   Guo, S., Dong, X., Wu, T., Shi, F., Zhu, C., 2015. Characteristic evolution of hydrochar from

16   hydrothermal carbonization of corn stalk. J. Anal. Appl. Pyrolysis.

17   https://doi.org/10.1016/j.jaap.2015.10.015

18   Haddad, K., Jeguirim, M., Jerbi, B., Chouchene, A., Dutournié, P., Thevenin, N., Ruidavets, L.,

19   Jellali, S., Limousy, L., 2017. Olive Mill Wastewater: From a Pollutant to Green Fuels,

20   Agricultural Water Source and Biofertilizer. ACS Sustain. Chem. Eng. 5, 8988–8996.

21   https://doi.org/10.1021/acssuschemeng.7b01786

22   Hao, S.W., Hsu, C.H., Liu, Y.G., Chang, B.K., 2016. Activated carbon derived from

23   hydrothermal treatment of sucrose and its air filtration application. RSC Adv.

1   https://doi.org/10.1039/c6ra23958g

2   Hodaifa, G., Ochando-Pulido, J.M., Rodriguez-Vives, S., Martinez-Ferez, A., 2013.

3   Optimization of continuous reactor at pilot scale for olive-oil mill wastewater treatment

4   by Fenton-like process. Chem. Eng. J. https://doi.org/10.1016/j.cej.2013.01.065

5   Hoekman, S.K., Broch, A., Robbins, C., 2011. Hydrothermal carbonization (HTC) of

6   lignocellulosic biomass. Energy and Fuels 25, 1802–1810.

7   https://doi.org/10.1021/ef101745n

8   Hu, L., Zhou, K., Li, Y., Chen, X., Liu, B., Li, C., Gong, X., Ma, F., 2018. Exogenous myo-

9   inositol alleviates salinity-induced stress in Malus hupehensis Rehd. Plant Physiol.

10   Biochem. https://doi.org/10.1016/j.plaphy.2018.10.037

11   Huang, N., Zhao, P., Ghosh, S., Fedyukhin, A., 2019. Co-hydrothermal carbonization of

12   polyvinyl chloride and moist biomass to remove chlorine and inorganics for clean fuel

13   production. Appl. Energy. https://doi.org/10.1016/j.apenergy.2019.02.050

14   Ibn Ferjani, A., Jeguirim, M., Jellali, S., Limousy, L., Courson, C., Akrout, H., Thevenin, N.,

15   Ruidavets, L., Muller, A., Bennici, S., 2019. The use of exhausted grape marc to produce

16   biofuels and biofertilizers: Effect of pyrolysis temperatures on biochars properties. Renew.

17   Sustain. Energy Rev. https://doi.org/10.1016/j.rser.2019.03.034

18   Organization Labor Organization, 2017. Olive and Olive oil production [WWW Document].

19   URL https://www.ilo.org/global/statistics-and-databases/lang--en/index.htm.

20   Agriculture/Sector/Olive and olive oil

21   International Organization for Standardization, G., 1995. 11261: Soil Quality: Determination

22   of Total Nitrogen: Modified Kjeldahl Method (ISO 11261:1995).

Jeguirim, M., Dutournié, P., Zorpas, A.A., Limousy, L., 2017. Olive Mill wastewater: From a pollutant to green fuels, agriculturalwater source and bio-fertilizer-part 1. The drying kinetics. Energies. https://doi.org/10.3390/en10091423

Jeguirim, M., Goddard, M.L., Tamosiunas, A., Berrich-Betouche, E., Azzaz, A.A., Praspaliauskas, M., Jellali, S., 2020. Olive mill wastewater: From a pollutant to green fuels, agricultural water source and bio-fertilizer. Biofuel production. Renew. Energy 149, 716–724. https://doi.org/10.1016/j.renene.2019.12.079

Jeguirim, M., Limousy, L., Dutournie, P., 2014. Pyrolysis kinetics and physicochemical properties of agropellets produced from spent ground coffee blended with conventional biomass. Chem. Eng. Res. Des. https://doi.org/10.1016/j.cherd.2014.04.018

Jiménez-Arias, D., García-Machado, F.J., Morales-Sierra, S., Luis, J.C., Suarez, E., Hernández, M., Valdés, F., Borges, A.A., 2019. Lettuce plants treated with L-pyroglutamic acid increase yield under water deficit stress. Environ. Exp. Bot. https://doi.org/10.1016/j.envexpbot.2018.10.034

Kammann, C., Ratering, S., Eckhard, C., Müller, C., 2012. Biochar and hydrochar eff ects on greenhouse gas (carbon dioxide, nitrous oxide, and methane) fluxes from soils. J. Environ. Qual. https://doi.org/10.2134/jeq2011.0132

Kanayama, Y., 2009. Physiological roles of polyols in horticultural crops. J. Japanese Soc. Hortic. Sci. https://doi.org/10.2503/jjshs1.78.158

Khiari, B., Wakkel, M., Abdelmoumen, S., Jeguirim, M., 2019. Dynamics and kinetics of cupric ion removal from wastewaters by Tunisian solid crude olive-oilwaste. Materials (Basel). https://doi.org/10.3390/ma12030365

Kim, J.H., Kannan, A.G., Woo, H.S., Jin, D.G., Kim, W., Ryu, K., Kim, D.W., 2015. A bi-

functional metal-free catalyst composed of dual-doped graphene and mesoporous carbon for rechargeable lithium-oxygen batteries. J. Mater. Chem. A. https://doi.org/10.1039/c5ta05334j

Komnitsas, K., Zaharaki, D., 2012. Pre-treatment of olive mill wastewaters at laboratory and mill scale and subsequent use in agriculture: Legislative framework and proposed soil quality indicators. Resour. Conserv. Recycl. https://doi.org/10.1016/j.resconrec.2012.09.009

Kruse, A., Dahmen, N., 2018. Hydrothermal biomass conversion: Quo vadis? J. Supercrit. Fluids 134, 114–123. https://doi.org/10.1016/j.supflu.2017.12.035

Krysanova, K., Krylova, A., Zaichenko, V., 2019. Properties of biochar obtained by hydrothermal carbonization and torrefaction of peat. Fuel. https://doi.org/10.1016/j.fuel.2019.115929

Lamer, V.K., Dinegar, R.H., 1950. Theory, Production and Mechanism of Formation of Monodispersed Hydrosols. J. Am. Chem. Soc. https://doi.org/10.1021/ja01167a001

Landriscini, M.R., Galantini, J.A., Duval, M.E., Capurro, J.E., 2019. Nitrogen balance in a plant-soil system under different cover crop-soybean cropping in Argentina. Appl. Soil Ecol. https://doi.org/10.1016/j.apsoil.2018.10.005

Li, M., Li, W., Liu, S., 2011. Hydrothermal synthesis, characterization, and KOH activation of carbon spheres from glucose. Carbohydr. Res. https://doi.org/10.1016/j.carres.2011.03.020

Li, R., Wang, L., Shahbazi, A., 2015. A Review of Hydrothermal Carbonization of Carbohydrates for Carbon Spheres Preparation. Trends Renew. Energy. https://doi.org/10.17737/tre.2015.1.1.009

Lin, Y., Ma, X., Peng, X., Yu, Z., 2016. A Mechanism Study on Hydrothermal Carbonization of Waste Textile. Energy and Fuels 30, 7746–7754. https://doi.org/10.1021/acs.energyfuels.6b01365

Lucas, M.S., Peres, J.A., 2009. Removal of COD from olive mill wastewater by Fenton's reagent: Kinetic study. J. Hazard. Mater. https://doi.org/10.1016/j.jhazmat.2009.03.002

Lucian, M., Volpe, M., Gao, L., Piro, G., Goldfarb, J.L., Fiori, L., 2018. Impact of hydrothermal carbonization conditions on the formation of hydrochars and secondary chars from the organic fraction of municipal solid waste. Fuel. https://doi.org/10.1016/j.fuel.2018.06.060

Méndez, A., Gascó, G., Ruiz, B., Fuente, E., 2019. Hydrochars from industrial macroalgae "Gelidium Sesquipedale" biomass wastes. Bioresour. Technol. https://doi.org/10.1016/j.biortech.2018.12.074

Moreno-Maroto, J.M., Uceda-Rodríguez, M., Cobo-Ceacero, C.J., de Hoces, M.C., MartínLara, M.Á., Cotes-Palomino, T., López García, A.B., Martínez-García, C., 2019. Recycling of 'alperujo' (olive pomace) as a key component in the sintering of lightweight aggregates. J. Clean. Prod. https://doi.org/10.1016/j.jclepro.2019.118041

Naisse, C., Girardin, C., Lefevre, R., Pozzi, A., Maas, R., Stark, A., Rumpel, C., 2015. Effect of physical weathering on the carbon sequestration potential of biochars and hydrochars in soil. GCB Bioenergy. https://doi.org/10.1111/gcbb.12158

Ovsyannikova, E., Arauzo, P.J., Becker, G., Kruse, A., 2019. Experimental and thermodynamic studies of phosphate behavior during the hydrothermal carbonization of sewage sludge. Sci. Total Environ. https://doi.org/10.1016/j.scitotenv.2019.07.217

Poerschmann, J., Baskyr, I., Weiner, B., Koehler, R., Wedwitschka, H., Kopinke, F.D., 2013a. Hydrothermal carbonization of olive mill wastewater. Bioresour. Technol. 133, 581–588.

https://doi.org/10.1016/j.biortech.2013.01.154

Poerschmann, J., Weiner, B., Baskyr, I, 2013b. Organic compounds in olive mill wastewater and in solutions resulting from hydrothermal carbonization of the wastewater. Chemosphere 92, 1472–1482. https://doi.org/10.1016/j.chemosphere.2013.03.061

Pulido, J.M.O., 2016. A review on the use of membrane technology and fouling control for olive mill wastewater treatment. Sci. Total Environ. https://doi.org/10.1016/j.scitotenv.2015.09.151

Qian, Y., Tan, D.X., Reiter, R.J., Shi, H., 2015. Comparative metabolomic analysis highlights the involvement of sugars and glycerol in melatonin-mediated innate immunity against bacterial pathogen in Arabidopsis. Sci. Rep. https://doi.org/10.1038/srep15815

R.K. Sairam, R.., Tyagi, A., Chinnusamy, V., 2006. Salinity tolerance: cellular mechanisms and gene regulation, in: Huang, B. (Ed.), Plant-Environment Interactions. CRC Press, pp. 121–175.

Ratcliff, A., Medley, E.E., Simmonds, P.G., 1974. Pyrolysis of amino acids. Mechanistic considerations. J. Org. Chem. https://doi.org/10.1021/jo00924a007

Ruiz, H.A., Rodríguez-Jasso, R.M., Fernandes, B.D., Vicente, A.A., Teixeira, J.A., 2013. Hydrothermal processing, as an alternative for upgrading agriculture residues and marine biomass according to the biorefinery concept: A review. Renew. Sustain. Energy Rev. https://doi.org/10.1016/j.rser.2012.11.069

Saba, A., Mcgaughy, K., Reza, M.T., 2019. Techno-Economic Assessment of Co-Hydrothermal Carbonization of a Coal-Miscanthus Blend 1–17. https://doi.org/10.3390/en12040630

Saha, N., Saba, A., Reza, M.T., 2019. Effect of hydrothermal carbonization temperature on pH, dissociation constants, and acidic functional groups on hydrochar from cellulose and wood. J. Anal. Appl. Pyrolysis. https://doi.org/10.1016/j.jaap.2018.11.018

Saqib, N.U., Baroutian, S., Sarmah, A.K., 2018. Physicochemical, structural and combustion characterization of food waste hydrochar obtained by hydrothermal carbonization. Bioresour. Technol. https://doi.org/10.1016/j.biortech.2018.06.112

Sedej, I., Milczarek, R., Wang, S.C., Sheng, R., de Jesús Avena-Bustillos, R., Dao, L., Takeoka, G., 2016. Membrane-Filtered Olive Mill Wastewater: Quality Assessment of the Dried Phenolic-Rich Fraction. J. Food Sci. https://doi.org/10.1111/1750-3841.13267

Sevilla, M., Fuertes, A.B., 2009. The production of carbon materials by hydrothermal carbonization of cellulose. Carbon N. Y. 47, 2281–2289. https://doi.org/10.1016/j.carbon.2009.04.026

Seyedsadr, S., Al Afif, R., Pfeifer, C., 2018. Hydrothermal carbonization of agricultural residues: A case study of the farm residues -based biogas plants. Carbon Resour. Convers. https://doi.org/10.1016/j.crcon.2018.06.001

Souilem, S., El-Abbassi, A., Kiai, H., Hafidi, A., Sayadi, S., Galanakis, C.M., 2017. Olive oil production sector: Environmental effects and sustainability challenges, in: Olive Mill Waste: Recent Advances for Sustainable Management. https://doi.org/10.1016/B978-0-12-805314-0.00001-7

T-412, 2012. Moisture in pulp , paper and paperboard. Stand. Off. Method, Tappi.

Theerakulpisut, P., Gunnula, W., 2012. Exogenous sorbitol and trehalose mitigated salt stress damage in salt-sensitive but not salt-tolerant rice seedlings. Asian J. Crop Sci. https://doi.org/10.3923/ajcs.2012.165.170

Thompson, W., Leege, P., 1998. Test methods for the examination of composting and compost. Commun. Soil Sci. Plant Anal.

Tisserat, B., Stuff, A., 2011. Stimulation of short-term plant growth by glycerol applied as foliar sprays and drenches under greenhouse conditions. HortScience. https://doi.org/10.21273/hortsci.46.12.1650

Ul Saqib, N., Sarmah, A.K., Baroutian, S., 2019. Effect of temperature on the fuel properties of food waste and coal blend treated under co-hydrothermal carbonization. Waste Manag. https://doi.org/10.1016/j.wasman.2019.04.005

Unur, E., Brutti, S., Panero, S., Scrosati, B., 2013. Nanoporous carbons from hydrothermally treated biomass as anode materials for lithium ion batteries. Microporous Mesoporous Mater. https://doi.org/10.1016/j.micromeso.2013.02.032

Volpe, M., Wüst, D., Merzari, F., Lucian, M., Andreottola, G., Kruse, A., Fiori, L., 2018. One stage olive mill waste streams valorisation via hydrothermal carbonisation. Waste Manag. 80, 224–234. https://doi.org/10.1016/j.wasman.2018.09.021

Wang, L., Chang, Y., Liu, Q., 2019. Fate and distribution of nutrients and heavy metals during hydrothermal carbonization of sewage sludge with implication to land application. J. Clean. Prod. https://doi.org/10.1016/j.jclepro.2019.03.347

Wang, T., Zhai, Y., Zhu, Y., Li, C., Zeng, G., 2018. A review of the hydrothermal carbonization of biomass waste for hydrochar formation: Process conditions, fundamentals, and physicochemical properties. Renew. Sustain. Energy Rev. https://doi.org/10.1016/j.rser.2018.03.071

Xiong, J. bo, Pan, Z. qian, Xiao, X. feng, Huang, H. jun, Lai, F. ying, Wang, J. xin, Chen, S. wei, 2019. Study on the hydrothermal carbonization of swine manure: The effect of

process parameters on the yield/properties of hydrochar and process water. J. Anal. Appl. Pyrolysis. https://doi.org/10.1016/j.jaap.2019.104692

Xue, Y., Gao, B., Yao, Y., Inyang, M., Zhang, M., Zimmerman, A.R., Ro, K.S., 2012. Hydrogen peroxide modification enhances the ability of biochar (hydrochar) produced from hydrothermal carbonization of peanut hull to remove aqueous heavy metals: Batch and column tests. Chem. Eng. J. https://doi.org/10.1016/j.cej.2012.06.116

Yalili Kiliç, M., Yonar, T., Kestioğlu, K., 2013. Pilot-scale treatment of olive oil mill wastewater by physicochemical and advanced oxidation processes. Environ. Technol. (United Kingdom). https://doi.org/10.1080/09593330.2012.758663

Yildizli, A., Çevik, S., Ünyayar, S., 2018. Effects of exogenous myo-inositol on leaf water status and oxidative stress of Capsicum annuum under drought stress. Acta Physiol. Plant. https://doi.org/10.1007/s11738-018-2690-z

Yu, K., Wang, J., Song, K., Wang, X., Liang, C., Dou, Y., 2019. Hydrothermal synthesis of cellulose-derived carbon nanospheres from corn straw as anode materials for lithium ion batteries. Nanomaterials. https://doi.org/10.3390/nano9010093

Zhang, L., Wang, Q., Wang, B., Yang, G., Lucia, L.A., Chen, J., 2014. Hydrothermal Carbonization of Corncob Residues for Hydrochar Production. https://doi.org/10.1021/ef502462p

Zhang, X., Gao, B., Fang, J., Zou, W., Dong, L., Cao, C., Zhang, J., Li, Y., Wang, H., 2019. Chemically activated hydrochar as an effective adsorbent for volatile organic compounds (VOCs). Chemosphere. https://doi.org/10.1016/j.chemosphere.2018.11.144

Zhao, P., Huang, N., Li, J., Cui, X., 2020. Fate of sodium and chlorine during the co-hydrothermal carbonization of high-alkali coal and polyvinyl chloride. Fuel Process.

Technol. 199, 106277. https://doi.org/10.1016/j.fuproc.2019.106277

Zirehpour, A., Jahanshahi, M., Rahimpour, A., 2012. Unique membrane process integration for olive oil mill wastewater purification. Sep. Purif. Technol. https://doi.org/10.1016/j.seppur.2012.05.028

Zuo, X.J., Liu, Z., Chen, M.D., 2016. Effect of H2O2 concentrations on copper removal using the modified hydrothermal biochar. Bioresour. Technol. https://doi.org/10.1016/j.biortech.2016.02.032